The Microwave Anisotropy Probe (MAP) Attitude Control System

F. Landis Markley, Stephen F. Andrews, James R. O'Donnell, Jr., David K. Ward, Aprille J. Ericsson

NASA's Goddard Space Flight Center, Greenbelt, MD, 20771, USA

Abstract

The Microwave Anisotropy Probe mission is designed to produce a map of the cosmic microwave background radiation over the entire celestial sphere by executing a fast spin and a slow precession of its spin axis about the Sun line to obtain a highly interconnected set of measurements. The spacecraft attitude is sensed and controlled using an Inertial Reference Unit, two Autonomous Star Trackers, a Digital Sun Sensor, twelve Coarse Sun Sensors, three Reaction Wheel Assemblies, and a propulsion system. This paper describes the design of the attitude control system that carries out this mission and presents some early flight experience.

Introduction

The Microwave Anisotropy Probe (MAP), the second Medium-Class Explorer (MIDEX) mission, was launched on June 30, 2001 as a follow-on to the Cosmic Background Explorer (COBE) satellite, which made unprecedented measurements of the Cosmic Microwave Background (CMB) that is believed to be a remnant of the Big Bang marking the birth of the universe. The Differential Microwave Radiometer (DMR) instrument on COBE made the first measurement of the anisotropy in the temperature of the CMB, other than the dipole due to the observer's motion.[1-4] MAP has been designed to measure this anisotropy with sensitivity 50 times that of DMR and angular resolution 30 times finer, specifically 20 microKelvin and 0.23°, respectively.[5] These increases in sensitivity and resolution will enable scientists to determine the values of key cosmological parameters and to answer questions about the formation of structure in the early universe and the fate of the universe.[6]

Since the major error sources in the DMR data arose from COBE's low Earth orbit, MAP was placed in a Lissajous orbit around the Sun-Earth L_2 Lagrange point to minimise magnetic, thermal, and radiation disturbances from the Earth and Sun. MAP attained its Lissajous orbit around L_2 in early October 2001, about 100 days after launch, using a lunar gravity assist with three phasing loops.[7] This paper will give an overview of the Attitude Control System (ACS) that acquires and maintains the spacecraft orbit, implements the spin-scan observing strategy described below, controls the spacecraft angular momentum, and provides for safety in the event of an anomaly. More detail can be found in References 8 and 9.

Observing Strategy

The MAP instrument includes radiometers at five frequencies, passively cooled to about 90°K, covering two fields of view (FOVs) 141° apart on the celestial sphere. The MAP observatory executes a fast spin at 0.464 rpm and a slower precession of its spin axis at one revolution per hour at a constant angle of 22.5° from the Sun line to obtain a highly interconnected set of measurements over an annulus between 87° and 132° from the Sun. Figure 1 shows the scan pattern covered by one of the two FOVs in one complete spacecraft precession (1 hour), displayed in ecliptic coordinates in which the ecliptic equator runs horizontally across the map. The bold circle shows the path for a single spin (2.2 minutes). As the Earth revolves around the Sun, this annulus of coverage revolves about the ecliptic pole. Thus the entire celestial sphere will be observed once every six months, as shown in Figure 2, or four times in the planned mission life of two years.

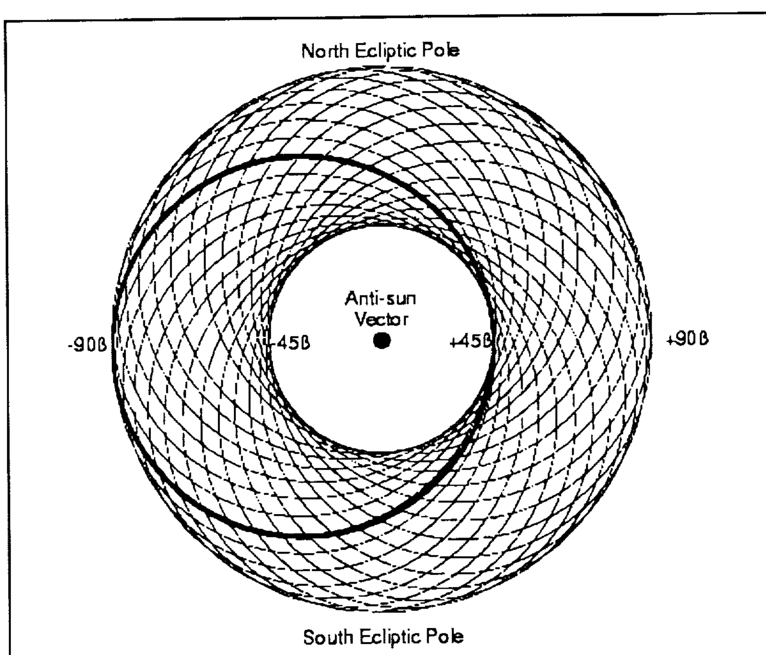

Figure 1: MAP Scan Pattern

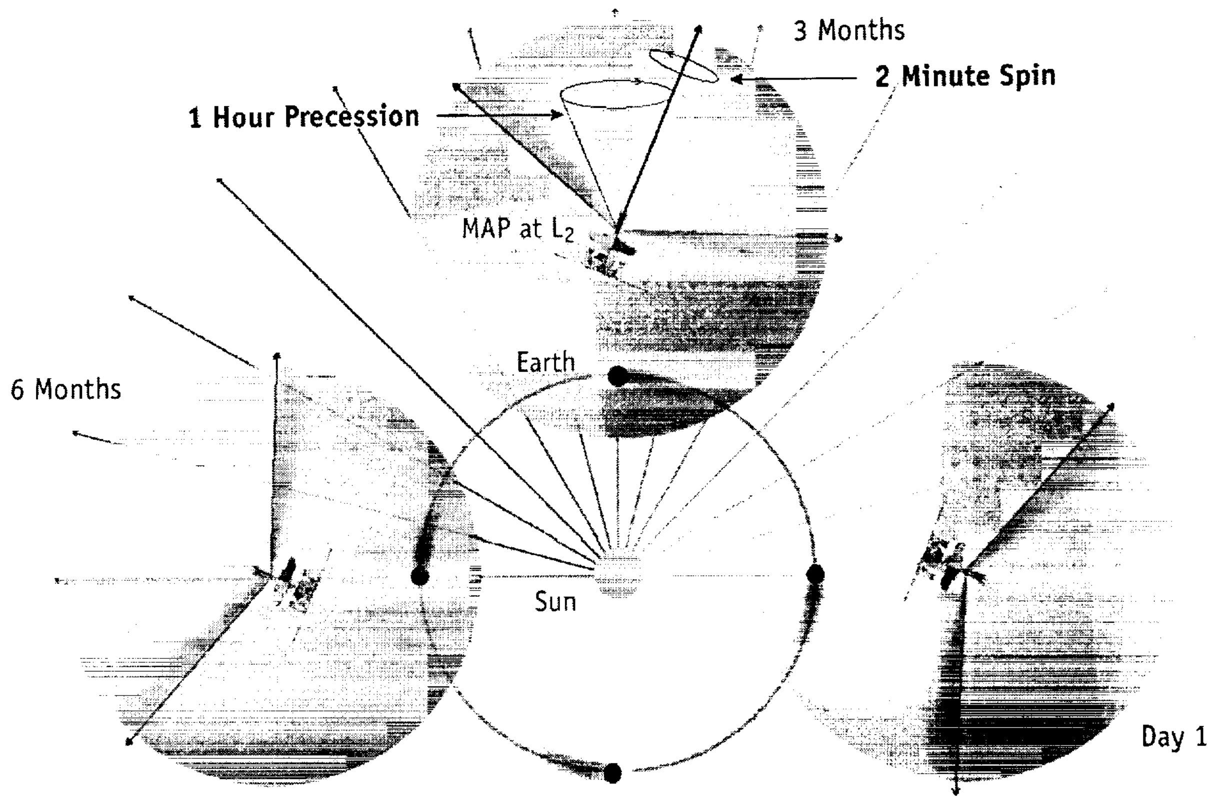

Figure 2: MAP Spin-Scan Concept

ACS Overview

The MAP ACS must implement the desired spin-scan motion and provide for orbit manoeuvres and safehold contingencies while minimising thermal and magnetic fluctuations, especially those synchronous with the spin period. The attitude sensors employed by MAP are an Inertial Rate Unit (IRU), two Autonomous Star Trackers (ASTs), a Digital Sun Sensor (DSS), and twelve Coarse Sun Sensors (CSSs). The spacecraft attitude is controlled by three Reaction Wheel Assemblies (RWAs), and a propulsion system. The ACS control algorithms are implemented in software in a Mongoose processor. Sensor data acquisition, actuator command processing, and an independent safehold algorithm are in the Attitude Control Electronics Remote Services Node (ACE RSN).

MAP uses three right-handed, orthonormal co-ordinate systems. The Geocentric Inertial frame (GCI) is an Earth-centred frame with its $\mathbf{x}_I$ axis pointing to the vernal equinox, its $\mathbf{z}_I$ axis pointing to the North Celestial Pole (parallel to the Earth's spin axis), and $\mathbf{y}_I = \mathbf{z}_I \times \mathbf{x}_I$. The Rotating Sun Referenced frame (RSR) is a spacecraft-centred frame in which the $\mathbf{z}_R$ axis points from the MAP spacecraft to the Sun, $\mathbf{x}_R$ is a unit vector in the direction of $\mathbf{z}_R \times \mathbf{z}_I$, and $\mathbf{y}_R = \mathbf{z}_R \times \mathbf{x}_R$. The RSR frame rotates at approximately 1°/day with respect to the GCI frame. The body frame is centred at the spacecraft centre of mass with $\mathbf{z}_B$ axis parallel to the spacecraft centreline, directed from the instrument to the solar arrays, $\mathbf{y}_B$ axis normal to the instrument radiator faces, and $\mathbf{x}_B = \mathbf{y}_B \times \mathbf{z}_B$, as shown in Figure 3.

The IRU comprises two Kearfott Two-Axis Rate Assemblies (TARAs), one with input axes aligned with the $\mathbf{z}_B$ and $\mathbf{x}_B$ axes and the other with input axes aligned with the $\mathbf{z}_B$ and $\mathbf{y}_B$ axes. This gives redundant rate inputs on the $\mathbf{z}_B$ axis; the DSS outputs can be differentiated to provide rates on the other axes in the event of an IRU failure.

The boresights of the two Lockheed-Martin ASTs are in the $\pm\mathbf{y}_B$ directions. Each AST tracks up to 50 stars simultaneously in its 8.8° square FOV, matches them to stars in an internal star catalogue, and computes its attitude as a GCI-referenced quaternion with accuracy of 21 arc-seconds (1σ) around its boresight axis and 2.3 arc-seconds (1σ) in the other two axes.

The Adcole two-axis DSS has two heads, each with 64° square FOV and an accuracy of 1 arc-minute (1σ). The centres of the FOVs of the two sensing heads are in the $\mathbf{x}_B$-$\mathbf{z}_B$ plane at angles of ±29.5° from the $\mathbf{z}_B$-axis. The CSSs are cosine eyes located in pairs looking outward from the edges of the six solar array panels, pointing alternately 36.9° up and 36.9° down from the $\mathbf{x}_B$-$\mathbf{y}_B$ plane.

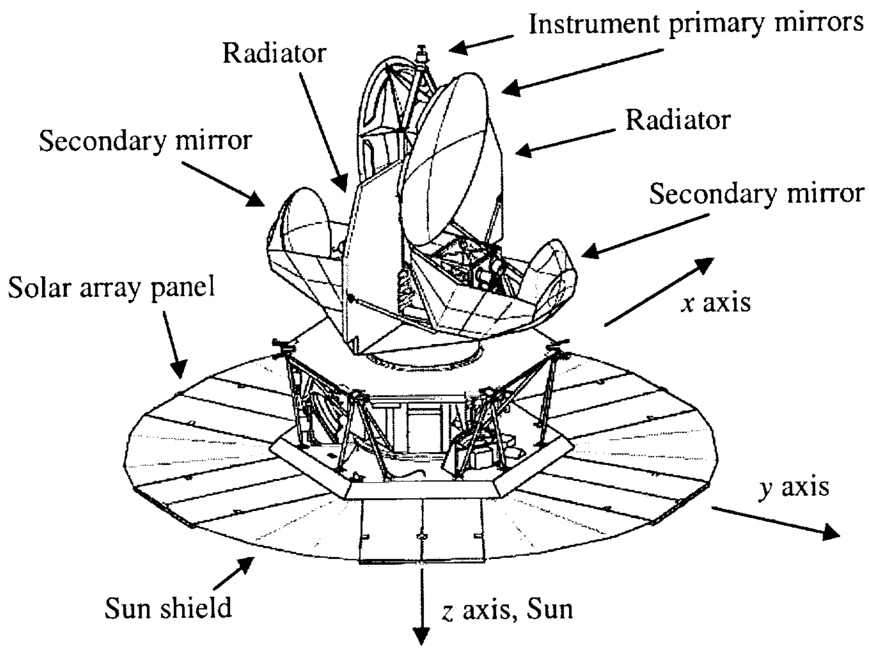

Figure 3: Spacecraft Layout and Body Coordinate Frame

The RWAs are Ithaco Type E wheels each with a momentum storage capacity of 80 Nms. The available reaction torque of each wheel is 0.3 Nm, but this is limited to 0.215 Nm by the MAP software to satisfy power constraints. The reaction wheel rotation axes are tilted 30° up from the $\mathbf{x}_B$-$\mathbf{y}_B$ plane (toward the instrument) and uniformly distributed 120° apart in azimuth about this axis. The wheels serve the dual function of counterbalancing the body's spin angular momentum to maintain the system momentum (i.e. body plus wheels) near zero while simultaneously applying control torques to provide the desired spacecraft attitude. The wheel axis orientations result in all wheel speeds being biased away from zero, thus avoiding zero-speed crossings that would obtain if the wheel spin axes were oriented along the spacecraft body frame co-ordinate axes.

The propulsion system comprises eight monopropellant hydrazine Reaction Engine Modules (REMs) and associated hardware. Each REM generates a maximum thrust of 4.45 N. The use of an L_2 orbit to avoid contamination by the Earth's magnetic field precludes the use of magnetic sensing or momentum unloading, since there is no appreciable magnetic field to perform these functions at L_2. Thus the propulsion system used to carry out the orbit manoeuvres to reach and maintain the L_2 orbit is also used to unload accumulated angular momentum from the reaction wheels. Gravity-gradient, atmospheric drag, and outgassing torques are significant in the phasing orbits prior to the lunar gravity assist; but the maximum accumulation of angular momentum from these sources is less than 1 Nms per orbit. Solar radiation pressure torque is the only significant disturbance torque at L_2, and the uniform rotation of the spin axis reduces its average torque by more than two orders of magnitude compared to its instantaneous value. Angular momentum due to these disturbances is stored in the reaction wheels and is only unloaded at the conclusion of an orbit manoeuvre, no more than once every three months at L_2. Pre-flight calculations of angular momentum accumulation from solar radiation pressure gave estimates ranging from 0.0016 Nms per day to 0.065 Nms per day, depending on the accuracy of deployment of the solar arrays and the resulting symmetry of the spacecraft.[9] The worst-case estimate gives an angular momentum accumulation to the Observing Mode limit of 2 N-m-s in 31 days, which would require use of the propulsion system for unloading more frequently than desired. Flight data indicates an angular momentum accumulation of less than 0.01 Nm per day, which meets the requirement of less than 2 Nms accumulation in three months.

ACS Operational Modes

There are six ACS operational modes: Observing, Inertial, Delta V, Delta H, Sun Acquisition, and Safehold. The first five modes are implemented in the Mongoose processor, while the Safehold Mode resides in the ACE. Figure 4 shows the modes and the transitions among them. Anomalous behaviour can result in autonomous transitions from any other mode to Safehold Mode or Sun Acquisition Mode, even though these transitions are not shown explicitly. The ACS modes are discussed below, including the sensors, actuators, and control algorithms used.

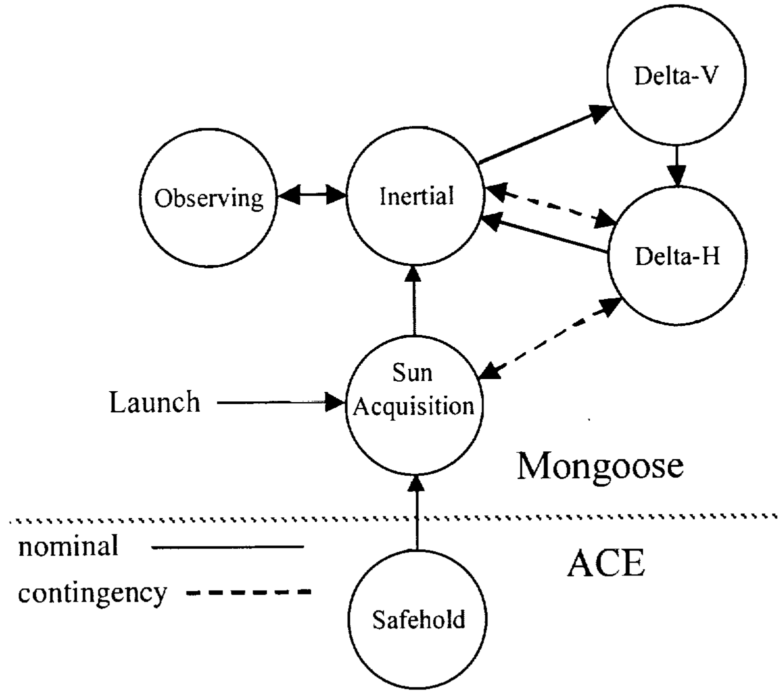

Figure 4: ACS Mode Transitions

Observing Mode

Observing Mode is used for science operations to maintain the 22.5°±0.25° angle between the spin axis and Sun line and to implement the observing strategy shown in Figures 1 and 2. This is accomplished by specifying the Observing Mode attitude of the MAP spacecraft with respect to the RSR co-ordinate frame by the set of 3-1-3 Euler angles[10, 11]

$$\phi_c = \phi_0 + \int_{t_0}^{t} \dot{\phi}_c dt, \qquad \theta_c = 22.5° = 0.3927 \text{ rad}, \qquad \text{and} \qquad \psi_c = \psi_0 + \int_{t_0}^{t} \dot{\psi}_c dt, \tag{1}$$

where $\dot{\phi}_c = 1 \text{ rev / hour} = 0.001745 \text{ rad / sec}$ and $\dot{\psi}_c = 0.464 \text{ rpm} = 0.04859 \text{ rad / sec}$ are the desired spin-scan rates, and ϕ_0 and ψ_0 are set by the initial state. A commanded RSR-to-body quaternion q_c and a commanded RSR-to-body angular rate vector $\boldsymbol{\omega}_c$ are computed from these Euler angles and rates by the standard equations.[10, 11]

The attitude error is expressed as two times the vector part $\mathbf{q}_e$ of an error quaternion q_e, which is the quotient of an estimated RSR-to-body quaternion $\hat{q}_{\mathrm{BR}}$ and the commanded quaternion:

$$q_e = \pm \hat{q}_{\mathrm{BR}} \otimes q_c^{-1}, \tag{2}$$

with the sign chosen so that the scalar component of q_e, which has magnitude close to unity for small pointing errors, is positive. The factor of two reflects the fact that the quaternion error is half the angle error when these are small. In this and the following we use the quaternion product convention of References 11 and 12 rather than that of Reference 10, so that the order of quaternion multiplication is the same as that of the corresponding direction cosine matrices. The estimated RSR-to-body quaternion $\hat{q}_{\mathrm{BR}}$ is computed as

$$\hat{q}_{\mathrm{BR}} = \hat{q}_{\mathrm{BI}} \otimes q_{\mathrm{RI}}^{-1}, \tag{3}$$

where the GCI-to-RSR quaternion q_{RI} is computed onboard from ephemeris models and the estimated GCI-to-body quaternion $\hat{q}_{\mathrm{BI}}$ is computed by an onboard Extended Kalman Filter (EKF) with IRU, AST, and DSS measurements as input.[12, 13] This filter is similar to EKFs employed on several previous missions, except that the AST produces an estimated attitude quaternion rather than merely observed star vectors, removing the burden on the Mongoose processor of star identification and the necessity to carry an onboard star catalogue. A rate error vector $\boldsymbol{\omega}_e$ is computed as

$$\boldsymbol{\omega}_e = \hat{\boldsymbol{\omega}}_{\mathrm{BI}} - \boldsymbol{\omega}_c, \tag{4}$$

where $\hat{\boldsymbol{\omega}}_{\mathrm{BI}}$ is the body rate measured by the IRU, corrected for gyro drifts that are also estimated by the EKF.

The RWA torques are computed by a proportional-derivative (PD) controller in terms of the attitude and rate errors.[14] A feedforward term is added to reduce hangoff error; this term includes both the angular acceleration required to follow the commanded attitude and the gyroscopic term required to move the system momentum $\mathbf{H}_{sys}$ in the body frame as required by its constancy in inertial space. Since $\dot{\phi}_c$, $\dot{\psi}_c$, and θ_c are all constant, the commanded acceleration is:

$$\dot{\boldsymbol{\omega}}_c = \dot{\psi}_c \dot{\phi}_c \sin\theta_c \begin{bmatrix} \cos\psi_c \\ -\sin\psi_c \\ 0 \end{bmatrix}. \tag{5}$$

The acceleration and gyroscopic terms are added to the commanded PD acceleration to give the total control torque:

$$\mathbf{T} = J\left[k_d \boldsymbol{\omega}_e + k_p(2\mathbf{q}_e) + \dot{\boldsymbol{\omega}}_c\right] + \boldsymbol{\omega}_c \times \mathbf{H}_{sys}, \tag{6}$$

where J is the MAP moment-of-inertia tensor and k_d and k_p are derivative and proportional gains. This torque is distributed to the RWAs using a torque distribution matrix defined by the orientation of the RWAs in the body co-ordinate system.

Inertial Mode

As shown in Figure 4, Inertial Mode acts as a staging mode between the other operations of the spacecraft. This is an RWA- and IRU-based mode similar to Observing Mode, using the same Kalman Filter, but differs in that the commanded rates are zero and the feedforward terms are absent. Inertial Mode can either hold the spacecraft in an inertially fixed orientation or slew the spacecraft to a sequence of GCI-to-body quaternions in a Command Quaternion Table (CQT) uploaded from the ground. A slew is executed if the desired orientation is not close to the current spacecraft orientation. Normal exits from Inertial Mode are by ground command only.

Delta V Mode

Delta V Mode, which uses the REMs to adjust the orbit in either the initial phasing loops or for L_2 stationkeeping, is only entered by ground commands from Inertial Mode. The commands include: (1) desired attitude for Delta V burn, specified as a single quaternion or a CQT, (2) burn start time, (3) burn duration, and (4) set of thrusters to be used for the Delta V. The spacecraft remains in Inertial Mode to slew from the initial orientation to the desired attitude for the start of the delta V, and transitions to Delta V Mode at the start time of the requested burn. The only sensors used in Delta V Mode are the IRU and RWA tachometers. This mode uses a PD controller to hold the spacecraft to a commanded quaternion attitude while executing the Delta V burn. The output of the controller is transformed into thruster firing commands using a pulse width modulator with a minimum pulse width of 0.04 sec. The desired attitude is held by off-pulsing the primary set of thrusters and on-pulsing the others. Normal exit is autonomously to Delta H Mode

Delta H Mode

Delta H Mode uses the REMs to unload spacecraft system angular momentum, which is computed using the IRU and RWA tachometers. It is used primarily upon exit from Delta V Mode; but entry can also be ground-commanded from Inertial Mode if necessary, although this is not anticipated. The same pulse width modulator is used for Delta H as for Delta V, with the exception that all thrusters are operated in an on-pulsing manner for Delta H. If entry was from Delta V or Inertial Mode, the ACS autonomously transitions to Inertial Mode after the momentum has been reduced to less than 0.3 Nms. Delta H Mode can also be entered from Sun Acquisition Mode, as discussed below, in which case the autonomous exit upon completion of the momentum unloading is back to Sun Acquisition Mode.

Sun Acquisition Mode

Sun Acquisition Mode uses the CSS, IRU, and RWAs to acquire and maintain a thermally safe power-positive orientation, with the spacecraft $\mathbf{z}_B$ axis within 25° of the Sun. Upon separation from the launch vehicle, the ACS is in Sun Acquisition Mode, which must slew the spacecraft from any initial angle and any initial body momentum less than [13, 13, 54] Nms to a power-positive orientation within 40 minutes. If the body momentum exceeds the amount that can be handled by the RWA-based Sun Acquisition Mode, the REM-based Delta H Mode is entered by ground command to reduce the momentum to an acceptable level, after which the spacecraft returns to Sun Acquisition Mode. Transition to Inertial Mode can be commanded after the Sun has been acquired and the attitude initialised. Transition to the Mongoose control modes from the ACE Safehold Mode is through Sun Acquisition Mode. If a failure of some component other than CSS and IRU occurs, an autonomous transition is made to Sun Acquisition Mode to slew the spacecraft to a safe attitude. Normal exit from Sun Acquisition Mode is by ground command to Inertial Mode.

Safehold Modes

The Safehold Mode is implemented in the ACE, so it can be entered in the event of a Mongoose anomaly. It has two configurations, which differ by the rate information used. The first, called Safehold IRU, is a copy of the Sun Acquisition Mode in the Mongoose. The second is a minimum-hardware Safehold Mode using only the RWAs and CSSs, with rate errors being computed by numerically differentiating the position error signals. Because it lacks body z rate information from the gyros, this mode can tolerate less system momentum than can the Sun Acquisition algorithm or Safehold IRU. Since the CSSs are insensitive to rotations about the Sun line, anti-runaway compensation is applied to prevent the wheels from uncontrolled spinning about the satellite's z-axis. This is accomplished by applying equal damping torques to the three wheels if the sum of their speeds exceeds a pre-set value, thereby suppressing z-axis rotation without applying a net torque in the x-y plane. Exit from either Safehold Mode is by ground command only.

Flight Experience

The Delta launch vehicle placed the spacecraft on a very accurate trajectory with body angular momentum of only 6.2 Nms. The latter is well within the capability of the Sun Acquisition Mode, which acquired the Sun within 15 minutes. Maximum pointing errors during the nine Delta V manoeuvres performed in the first three months of the mission were smaller than predicted (3.7° vs. 5.5°), and imparted velocity increments were accurate to 1%. Less than 15 kg of hydrazine propulsion fuel was expended to get to L_2, about half the amount that was budgeted for this phase of the mission. The 57 kg of fuel remaining for stationkeeping and momentum unloading at L_2 will easily support a four-year extended mission.

Initially, the precession rate $\dot{\phi}$ in Observing Mode did not meet its 5% accuracy requirement, showing a 7% variation at the spin period. This problem was attributed to an inaccurate value of system momentum in the gyroscopic feedforward loop arising from a scale factor error in the RWA tachometer signals. Evidence for this was that the magnitude of the system momentum, which should be constant, had a 0.4 Nms oscillation at spin period and increased during spin-up by 1.0 Nms. Comparing a high-fidelity simulation with flight data determined that the oscillation and spin-up offset could be removed by a small change in the tachometer scale factor for each wheel: about 2.5% for RWA1 and about 4% for RWA2 and RWA3. After loading these new scale factors, the variation of the precession rate was dramatically reduced, as were the spin-period oscillation and the spin-up offset in the computed system momentum magnitude shown in Figure 5.

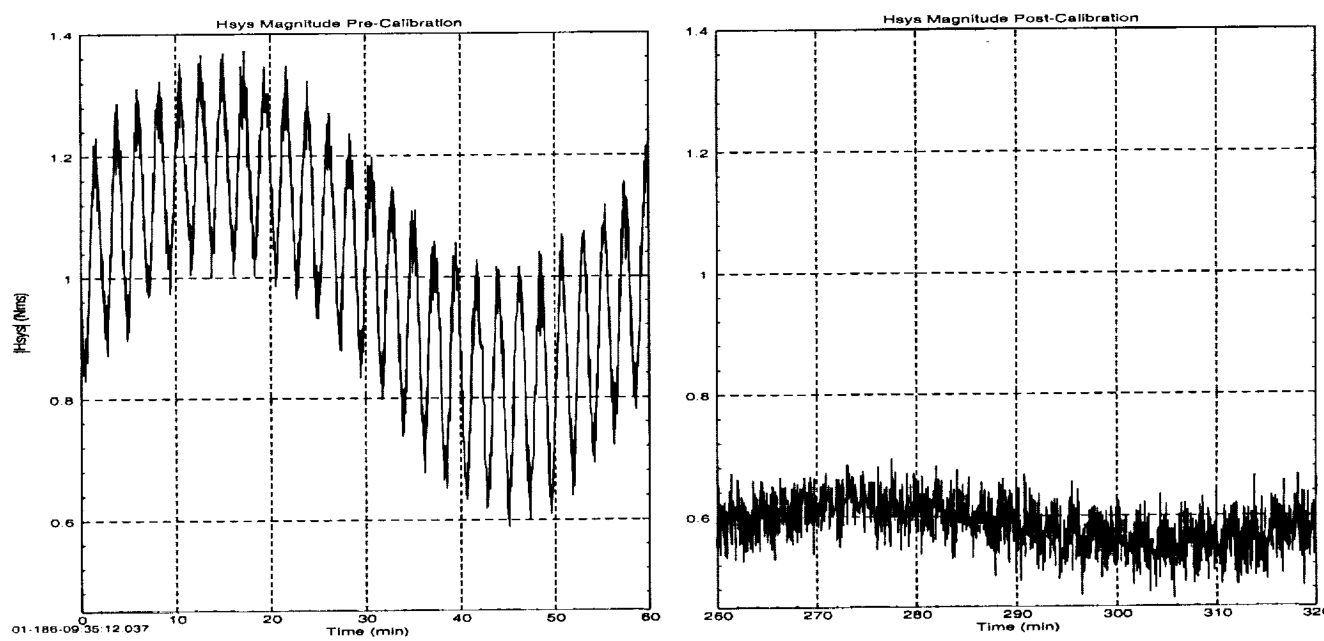

Figure 5: Pre- and Post-Calibration System Angular Momentum Magnitude

Stray light and radiation interference in the ASTs during the phasing loops was less of a problem than anticipated. Both ASTs lost track when the Moon was within a degree or so of the FOV, but only for a few seconds in a spin cycle, and only for three spin cycles in any precession cycle; only 13 AST readings were lost in a precession cycle. There is no Moon, Earth, or Sun interference at L_2, and the ASTs have been routinely tracking 15 to 40 stars in the absence of interference. Attitude knowledge has been better than 20 arc seconds per axis, easily meeting the three-axis root-sum-square requirement of 78 arc seconds. The Sun angle has been maintained between 22.44° and 22.54° in Observing Mode, as illustrated by the perfect circle traced by the Sun vector over several hours in Figure 6.

Charged particle flux from extreme solar activity on November 5 caused a power-on reset of the Mongoose processor. The ACS transitioned autonomously to Safehold Mode in the ACE, which functioned exactly as designed to keep MAP safe. The transition to Safehold Mode was discovered by operations staff at the next telemetry pass about 12 hours later, and recovery to Observing Mode was accomplished within three hours of this discovery.

Conclusions

The attitude control system described in this paper has successfully met the demanding requirements of the Microwave Anisotropy Probe mission. These include the need to function robustly far from the Earth where no magnetic field is useful for sensing or actuation, and with infrequent telemetry passes. The processor upset on November 5 illustrated the importance of having a safemode control capability that is independent of the primary control hardware and software.

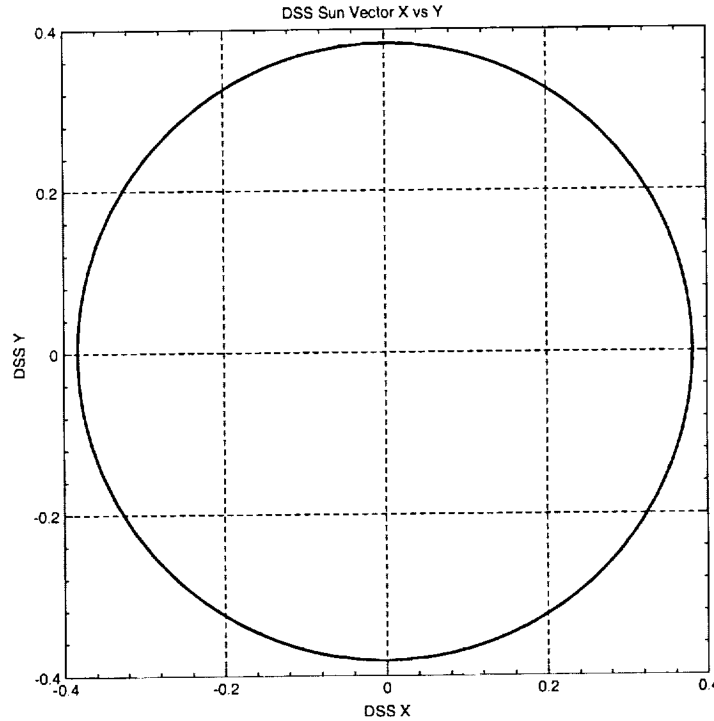

Figure 6: DSS Measurements in Observing Mode

References

1. Boggess, N. W., *et al.*, The *COBE* Mission: Its Design and Performance Two Years After Launch, *Astrophysical Journal*, vol. 397, no.2, pp. 420-429, 1992
2. Gulkis, S., Lubin, P. M., Meyer, S. S., and Silverberg, R. F., The Cosmic Background Explorer, *Scientific American*, vol.262, no.1, pp.132-139, 1990
3. Smoot, G. F., *et al.*, Structure in the *COBE* Differential Microwave Radiometer First-Year Maps, *Astrophysical Journal Letters*, vol.396, pp.L1-L5, 1992
4. Bennett, C.L., *et al.*, Four-Year *COBE* DMR Cosmic Microwave Background Observations: Maps and Basic Results, *Astrophysical Journal Letters*, vol.464, pp.L1-L4, 1996.
5. Bennett, C. L., Hinshaw, G. F., and Page L., A Cosmic Cartographer, *Scientific American*, vol.284, no.1, pp.44-45, 2001 (see also http://map.gsfc.nasa.gov)
6. Hu, W., Sugiyama, N., and Silk, J., The Physics of Microwave Background Anisotropies, *Nature*, vol.386, no.6620, pp. 37-43, 1997 (see also http://background.uchicago.edu)
7. Richon, K. V., and Mathews, M. W., An Overview of the Microwave Anisotropy Probe (MAP) Trajectory Design, *Astrodynamics 1997*, Volume 97, *Advances in the Astronautical Sciences*, edited by F. R. Hoots, B. Kaufman, P. J. Cefola, and D. B. Spencer, San Diego, CA, Univelt, Inc. for the American Astronautical Society, pp. 1979-1998, 1998
8. Andrews, S. F., Campbell, C. E., Ericsson-Jackson, A. J., Markley, F. L., and O'Donnell, J. R., MAP Attitude Control System Design and Analysis, *Flight Mechanics Symposium 1997*, NASA CP-3345, Greenbelt, MD, pp.445-456, 1997
9. Ericsson-Jackson, A. J., Andrews, S. F., O'Donnell, J. R., Jr., and Markley, F. L., MAP Stability, Design and Analysis, *Spaceflight Dynamics 1998*, Volume 100, *Advances in the Astronautical Sciences*, edited by Thomas H. Stengle, San Diego, CA, Univelt, Inc. for the American Astronautical Society, pp. 955-969, 1998
10. Wertz, J. R., ed., *Spacecraft Attitude Determination and Control*, Dordrecht, Holland, D. Reidel, 1978
11. Shuster, M. D., A Survey of Attitude Representations, *Journal of the Astronautical Sciences*, vol.41, no.4, pp.439-517, 1993
12. Lefferts, E. J., Markley, F. L., and Shuster, M. D., Kalman Filtering for Spacecraft Attitude Estimation, *Journal of Guidance, Control, and Dynamics*, vol.5, no.5, pp.417-429, 1982
13. Murrell, J. W., Precision Attitude Determination for Multimission Spacecraft, *1978 AIAA Guidance and Control Conference*, AIAA Paper 78-1248, Palo Alto, CA, pp.70-87, 1978
14. Wie, B., and Barba, P. M., Quaternion Feedback for Spacecraft Large Angle Maneuvers, *Journal of Guidance, Control, and Dynamics*, vol.8, no.3, pp.360-365, 1985